



Modeling and Hybrid Pareto Optimization of Cyclone Separators Using Group Method of Data Handling (GMDH) and Particle Swarm Optimization (PSO)

M. J. Mahmoodabadi^a, M. Taherkhorsandi^b, H. Safikhani^c

^a Department of Mechanical Engineering, Sirjan University of Technology, Sirjan, Iran

^b Young Researchers Club, Rasht branch, Islamic Azad University, Rasht, Iran

^c Department of Mechanical Engineering, Amirkabir University of Technology, Tehran, Iran

PAPER INFO

Paper history:

Received 05 January 2012

Accepted in revised form 30 August 2012

Keywords:

Two-phase Flow

Gas-solid

Particle Swarm Optimization

Multi-objective Optimization

GMDH

ABSTRACT

In the present study, a three-step multi-objective optimization algorithm of cyclone separators is utilized for the design objectives. First, the pressure drop (Δp) and collection efficiency (η) in a set of cyclone separators are numerically evaluated. Secondly, two meta models based on the evolved Group Method of Data Handling (GMDH) type neural networks are regarded to model the Δp and η as the required functions of geometrical characteristics. Finally, a multi-objective (MO) algorithm based on hybrid of Particle Swarm Optimization (PSO), multiple crossover and mutation operator are used for Pareto based optimization of cyclones considering two conflicting objectives Δp and η . By comparing the Pareto results of MOPSO with that of multi-objective genetic algorithms (NSGA II) regarding Pareto based multi-objective optimization of the obtained polynomial meta-models, it is shown that there are some interesting and important relationships as useful optimal design principles involved in the performance of cyclone separators.

doi: 10.5829/idosi.ije.2013.26.09c.15

NOMENCLATURE

u	velocity
x	position
P	pressure
N_c	number of effective turns
V_{in}	inlet velocity
VP	velocity pressure
Y	Inlet width
X	Inlet height
R	Reynolds stress tensor
D_{50}	Cut-point
*	set of decision variables
\mathbb{F}^*	set of objective functions

Greek Symbols

ρ	density
ν	viscosity

Subscripts

p	particle
i,j,k	1,2,3
t	turbulent

Superscripts

-	mean variables
---	----------------

1. INTRODUCTION

Cyclones are widely used in filtration and separation industry because of their simple setup and low cost maintenance. A number of studies were provided which

some of them can be more concerned. Stairmand [1] presented one of the most popular design tools which suggested that the cylinder height and exit tube length are 1.5 and 0.5 times of the cyclone body diameter for the design of a high efficiency cyclone, respectively. Leith et al. [2] and Bhatia et al. [3] discussed the effects of the cone opening size on pressure drop and collection efficiency. Zhu et al. [4] conducted detailed experiments

*Corresponding Author Email: mahmoodabadi@sirjantech.ac.ir (M. J. Mahmoodabadi)

on cyclones of different height and different vortex finder length and found that like other important dimensions such as body diameter and gas exit tube diameter, the cyclone height and vortex finder length can considerably influence the separation efficiency of the cyclones. Ravi et al. [5] investigated an MO optimization process on cyclone separators by using the NSGA algorithm. They tried to minimize the pressure drop and maximize the collection efficiency in cyclone separators. They did not use CFD in their optimization procedure and used analytical function for pressure drop and collection efficiency. Rongbiao et al. [6] suggested that the flow rate has a strong influence on the collection efficiency and the reduction in cone size results in higher collection efficiency without significant increase of pressure drop. Shalaby et al. [7] used Large Eddy Simulation (LES) for CFD modeling of gas-solid flow in cyclones and they obtained good compatibility with experimental results. Safikhani et al. [8] obtained detailed flow information by CFD simulation for three standard cyclone separators with different geometries. They discussed the effects of different geometrical parameters on the pressure drop and collection efficiency. Safikhani et al. [9] investigated an MO optimization algorithm on cyclones using genetic algorithms. They finally determined 5 optimum cyclones which had minimum pressure drop and maximum collection efficiency.

Both pressure drop and collection efficiency in cyclones are important objective functions which must be optimized simultaneously in such a real world complex multi-objective optimization problem. These objective functions are either obtained from experiments or computed using very timely and high-cost Computational Fluid Dynamic (CFD) approaches, which cannot be used in an iterative optimization task unless a simple but effective meta-model is constructed over the response surface from the numerical or experimental data. Therefore, in the present study, modeling and optimization of the parameters are investigated by using Grouped Method of Data Handling (GMDH) type neural networks and Multi-Objective Particle Swarm Optimization method (MOPSO) in order to minimize the pressure drop and maximize the collection efficiency.

System identification and modeling of complex processes using input-output data have always attracted many research efforts. In fact, system identification techniques are applied in many fields in order to model and predict the behavior of unknown and/or very complex systems based on given input-output data [10]. In this way, soft-computing methods [11] which concern computation in an imprecise environment, have gained significant attention. The main components of the soft computing, namely, fuzzy logic, neural network, and evolutionary algorithms have shown great ability in solving complex non-linear system

identification and control problems. Many research efforts have been expended to make use of evolutionary methods as effective tools for system identification [12]. Among these methodologies, Group Method of Data Handling (GMDH) algorithm is a self-organizing approach by which models of growing complexity are generated based on the evaluation of their performances on a set of multi-input-single-output data pairs (X_i, Y_i) ($i=1, 2, \dots, M$). The GMDH was first developed by Ivakhnenko [13] as a multivariate analysis method for modeling and identification of complex systems which can be used to model complex systems without having specific knowledge of the systems. The main idea of GMDH is to build an analytical function in a feed forward network based on a quadratic node transfer function [14] whose coefficients are obtained by using the regression technique. In recent years, however, the use of such self-organizing networks leads to successful application of the GMDH-type algorithm in a broad range of areas in engineering, science, and economics.

Particle Swarm Optimization (PSO), first introduced by Kennedy et al. [15], is one of the modern heuristic algorithms. It was developed through simulation of a simplified social system, and has been found to be robust in solving continuous nonlinear optimization problems [15-16]. The PSO technique can generate a high-quality solution within short calculation time and stable convergence characteristic as compared with other stochastic methods [17-18]. In this paper, for increasing the convergence of the population and to escape the local minima, PSO is merged with multiple crossover and mutation operator. Furthermore, over the last decade, the multi-objective PSO has been utilized to solve various types of multi-objective engineering optimization problems [19-21].

In the present study, firstly, the pressure drop (Δp) and the collection efficiency (η) in a set of cyclones are numerically investigated by using CFD techniques. Next, GMDH type neural networks are used to obtain polynomial models for the effects of geometrical parameters of the cyclones on both Δp and η . Finally, the obtained simple polynomial models are used in a Pareto based MOPSO to find the best possible combinations of Δp and η , known as the Pareto front. The Pareto results of MOPSO are also compared with that of multi-objective genetic algorithms (NSGAI).

2. THE CFD SIMULATION AND VALIDATION OF THE RESULTS

2.1. The CFD Simulation The CFD simulations are performed by using FLUENT. Inlet mass flow boundary condition is used at the cyclone inlet and a fully developed boundary condition is used at the outlet [8, 22]. The SIMPLE method is used for the pressure-

velocity coupling. Turbulence fluctuations are simulated by using Reynolds Stress Transport Model (RSTM) due to its accuracy [23], and velocity fluctuations are simulated by using the discrete random walk (DRW). The Lagrangian method is used for tracking of the particles in the simulations; and grid refinement tests are conducted in order to make sure that the solutions do not dependent on the grid. Collection efficiency statistics are obtained by releasing a specific number of particles at the inlet of the cyclones and by monitoring the number escaping through the underflow. The range of particles size is 0.1-10 μm of a material whose density is equal to 2500 kg/m^3 . The computation continues until the solutions converge into a total residue of less than 0.0001.

To test for grid independency, three grid types with increasing grid density are studied. The computational results of 3 grid types are compared in Table 1. It was observed that the maximum difference among the results is less than 4%, so that the grid template 186,222 is used for all computations in the present study. Figure 1 shows the details of the computational grid for the cyclones.

2. 2. The Definition of the Objective Functions

The pressure drop and collection efficiency in cyclones are important objective functions which have to be optimized simultaneously. The collection efficiency statistics are obtained by releasing a specified number of particles at the inlet of the cyclones and by monitoring the number escaping through the underflow. The first theory for collection efficiency in conventional cyclones was developed by Shepherd et al. [24]. It is based on the assumption of a plug flow. In order to calculate the efficiency, first the particle size with 50% collection efficiency ($D_{p50\%}$) needs to be determined according to the following equation:

$$D_{p50\%} = \sqrt{\frac{9\mu Y}{2\pi N_e V_{in} \rho_p}} \tag{1}$$

The collection efficiency for any other particle size (D_{pj}) can then be determined by:

$$\eta = \frac{1}{1 + \left(\frac{D_{p50\%}}{D_{pj}}\right)^2} \tag{2}$$

Many empirical models have been proposed for the pressure drop in the conventional cyclones [24-27]. In Wang's model, the total pressure loss in the cyclone is obtained by summing up the five pressure drop components as follows:

$$\Delta P_{total} = \Delta P_e + \Delta P_k + \Delta P_f + \Delta P_r + \Delta P_o \tag{3}$$

where, the components of Equation (3) are explained in Table 2.

2. 3. Definition of the Design Variables The design variables in the present paper are: the dimensionless length of vortex finder (S/D), dimensionless diameter of vortex finder (D_e/D), dimensionless length of upside cyclone (L_{up}/D) and dimensionless length of downside cyclone (L_{Down}/D). The design variables and their range of variations are shown in Figure 2 and Table 3, respectively. The different design variables are selected by dividing (S/D), (D_e/D), (D_{up}/D), and (D_{Down}/D) into 3 equal parts. By changing the geometrical independent parameters according to Table 3, various designs will be generated and evaluated by CFD. Consequently, some meta-models can be optimally constructed by using the GMDH type neural networks, which will be further used for the multi-objective Pareto based design of such cyclones.

TABLE 1. The comparison of the dimensionless pressure drop and the collection efficiency for 3 different grid numbers.

Total No. of Cells	$\Delta p / 0.5v^2$	η (%)
186,222	10.98	53.07
202,318	11.02	51.42
284,756	11.13	53.12
Max Diff (%)	1.348	3.200

TABLE 2. The components of Wang's pressure drop theory.

Component	Definition
$\Delta P_e = C_2 VP_{in}$	Entry loss, $C_2 \approx 1$
$\Delta P_k = VP_{in} - VP_{out}$	Kinetic Energy Loss
$\Delta P_f = C VP_{in}$	Frictional Loss, $C_{1D3D} = 0.14, C_{2D2D} = 0.28, C_{1D2D} = 0.15$
$\Delta P_r = \rho V_{in}^2 (R/r_0 - 1)$	Rotational loss, r_0 =radius of the vortex interface, R =cyclone body radius
$\Delta P_o = C_3 VP_{out}$	Pressure loss in the inner vortex and exit tube, $C_3 \approx 1.8$

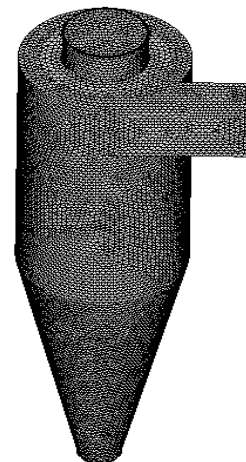


Figure 1. The details of the computational grid for the cyclones

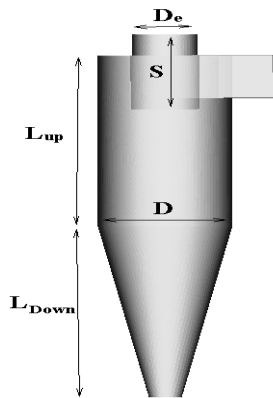


Figure 2. Design variables for the cyclone-optimization problems

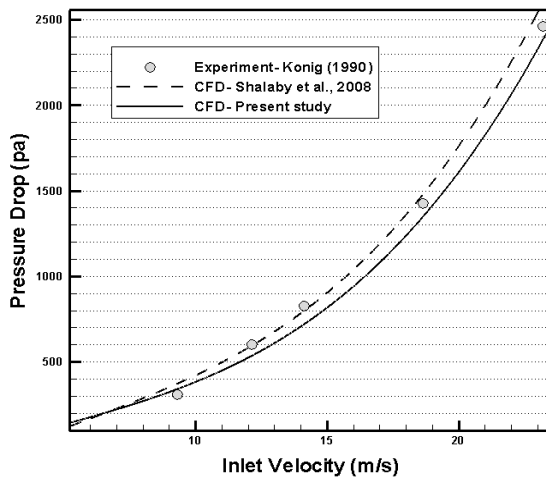


Figure 3. The comparison of CFD prediction and experimental data of Konig [28] for pressure drop.

TABLE 3. Design variables and their range of variations

Design Variable	From	To
S/D	0.900	1.725
D_c/D	0.125	0.600
L_{up}/D	0.875	2.775
L_{Down}/D	0.875	2.775

2. 4. Validation of the CFD Results To attain the confidence about the simulation, it is necessary to compare the simulation result with the available data. The comparison of CFD prediction and experimental data of Konig [28] for the pressure drop is shown in Figure 3. As seen, our numerical procedure predicts the pressure drop with the acceptable deviation from the experimental data of Konig [28] and CFD simulations of Shalaby et al. [7], but with increasing the flow rate differences of numerical prediction and experimental

data. This numerical error could contribute and cause the increase of flow complexity in high flow rates.

The comparison of CFD prediction and experimental data of Konig [28] for collection efficiency is shown in Figure 4. It is obvious that our numerical simulations can properly adapt with the pattern of experimental efficiency curve.

Tangential and axial velocities are important factors for the particle collection in the cyclones. Figures 5 and 6 compare the tangential and axial velocity of CFD prediction and experimental data. As seen, the CFD curves of the present study agree well with the experimental data of Fraser et al. [29] and the CFD simulations of Shalaby et al. [7]. Samples of numerical results obtained by using CFD are shown in Table 4; moreover, the velocity vector and pressure contour in one of these CFD simulations are shown in Figure 7.

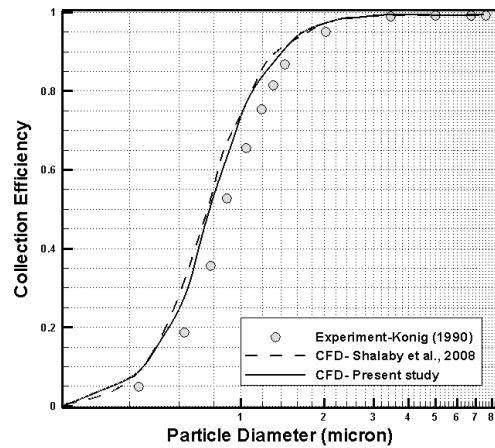


Figure 4. The comparison of CFD prediction and experimental data of Konig [28] for collection efficiency.

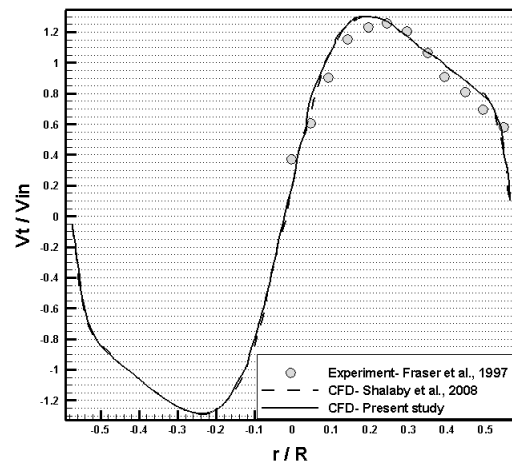


Figure 5. Comparison between the tangential velocity of CFD prediction and experimental data.

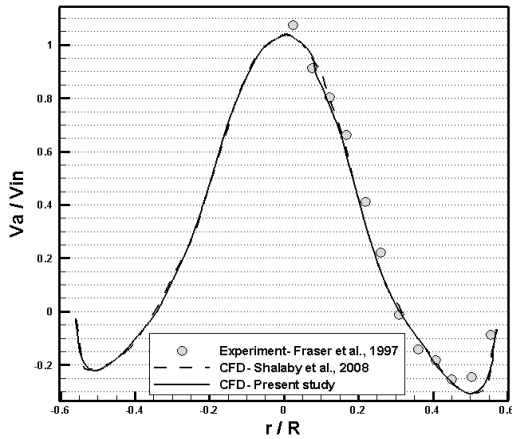


Figure 6. The comparison between the axial velocity of CFD prediction and experimental data.

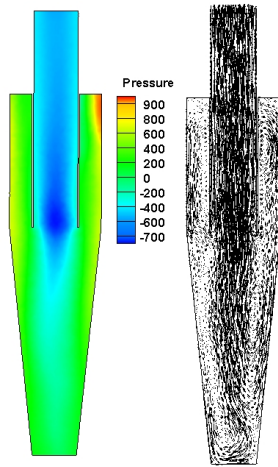


Figure 7. The velocity vector and pressure contour in the CFD simulations.

TABLE 4. Samples of numerical results obtained by using CFD.

Num	Input Data				Output Data	
	S/D	D _c /D	L _{up} /D	L _{down} /D	Δp / 1.5ρ v ²	η (%)
1	0.900	0.125	0.875	0.875	13.155	83.775
2	1.325	0.125	1.500	0.875	15.121	88.801
3	1.725	0.125	0.875	1.500	14.486	90.921
4	1.725	0.125	1.500	1.500	14.051	89.103
5	1.725	0.125	2.775	1.500	11.944	85.539
6	0.900	0.600	0.875	2.775	7.801	44.594
7	1.725	0.600	1.500	2.775	9.574	49.940
8	0.900	0.250	1.500	2.775	8.697	48.028
9	0.900	0.250	2.775	2.775	7.393	46.099
10	1.325	0.250	2.775	2.775	8.760	49.862
...
80	1.725	0.250	2.775	2.775	9.354	52.689
81	1.725	0.600	2.775	2.775	8.138	47.943

The results obtained in such CFD analysis can now be used to build the response surface of both collection efficiency and pressure drop for those different 81 geometries using GMDH type polynomial neural networks. Such meta-models will, in turn, be used for the Pareto-based multi-objective optimization of the cyclones. A post analysis using CFD is also performed to verify the optimum results by using the meta-modeling approach. Finally, the solutions obtained by the approach of this paper exhibit some important trade-offs among those objective functions which can be simply used by a designer to optimally compromise among the obtained solutions.

3. MODELING OF PRESSURE DROP AND COLLECTION EFFICIENCY USING GMDH TYPE NEURAL NETWORKS

By means of the GMDH algorithm, a model can be represented as a set of neurons in which different pairs of them in each layer are connected through a quadratic polynomial and thus produce new neurons in the next layer. Such representation can be used in modeling to map inputs to outputs. The formal definition of the identification problem is to find a function \hat{f} that can be approximately used instead of actual one f in order to predict output \hat{y} for a given input vector $X = (x_1, x_2, x_3, \dots, x_n)$ as close as possible to its actual output y . Therefore, given M observations of multi-input-single-output data pairs so that

$$y_i = f(x_{i1}, x_{i2}, x_{i3}, \dots, x_{in}) \quad (i=1, 2 \dots M) \tag{4}$$

It is now possible to train a GMDH-type neural network to predict the output values \hat{y}_i for any given input vector $X = (x_{i1}, x_{i2}, x_{i3}, \dots, x_{in})$, that is

$$\hat{y}_i = \hat{f}(x_{i1}, x_{i2}, x_{i3}, \dots, x_{in}) \quad (i=1, 2 \dots M) \tag{5}$$

The problem is now to determine a GMDH-type neural network so that the square of difference between the actual output and the predicted one is minimized, that is:

$$\sum_{i=1}^M [\hat{f}(x_{i1}, x_{i2}, x_{i3}, \dots, x_{in}) - y_i]^2 \rightarrow \min \tag{6}$$

General connection between input and output variables can be expressed by a complicated discrete form of Volterra functional series in the following form:

$$y = a_0 + \sum_{i=1}^n a_i x_i + \sum_{i=1}^n \sum_{j=1}^n a_{ij} x_i x_j + \sum_{i=1}^n \sum_{j=1}^n \sum_{k=1}^n a_{ijk} x_i x_j x_k + \dots \tag{7}$$

which is known as the Kolmogorov-Gabor polynomial [14]. This full form of mathematical description can be represented by a system of partial quadratic polynomials consisting of only two variables (neurons) in the following form:

$$\hat{y} = G(x_i, x_j) = a_0 + a_1 x_i + a_2 x_j + a_3 x_i x_j + a_4 x_i^2 + a_5 x_j^2 \quad (8)$$

There are two main concepts involved within GMDH-type neural networks design, namely, the parametric and the structural identification problems. In this way, some works by Jamali et al. [30] present a hybrid GA and singular value decomposition (SVD) method to optimally design such polynomial neural networks. The methodology in these references has been successfully used in this paper to obtain the polynomial models of Δp and η . The obtained GMDH-type polynomial models have shown to have quite suitable prediction ability of unforeseen data pairs during the training process. This will be presented in the following sections.

The input–output data pairs used in such modeling involve two different data tables obtained from CFD simulation discussed in Section 2. Both tables consist of four variables as inputs, namely (S/D) , (D_e/D) , (L_{up}/D) and (L_{Down}/D) and outputs which are Δp and η . The tables consist of a total of 81 patterns, which have been obtained from the numerical solutions to train and test such GMDH type neural networks. However, in order to demonstrate the prediction ability of the evolved GMDH type neural networks, the data in both input–output data tables have been divided into two different sets, namely, training and testing sets. The training set, which consists of 61 out of the 81 input–output data pairs for Δp and η , is used for training the neural network models using the method presented in Section 2. The testing set, which consists of 20 unforeseen input–output data samples for Δp and η during the training process, is merely used for testing to show the prediction ability of such evolved GMDH type neural network models. The GMDH type neural networks are now used for such input–output data to find the polynomial models of Δp and η with respect to their effective input parameters. In order to genetically design such GMDH type neural networks described in the previous section, a population of 10 individuals with a crossover probability (P_c) of 0.7 and mutation probability (P_m) 0.07 has been used in the 500 generations for Δp and η . The corresponding polynomial representation for dimensionless pressure drop is as follows:

$$Y_1 = 15.20 - 16.69 \left(\frac{D_e}{D}\right) + .22 \left(\frac{L_{up}}{D}\right) + 13.68 \left(\frac{D_e}{D}\right)^2 - .41 \left(\frac{L_{up}}{D}\right)^2 + .55 \left(\frac{D_e}{D}\right) \left(\frac{L_{up}}{D}\right) \quad (9.a)$$

$$Y_2 = 6.52 + 10.92 \left(\frac{S}{D}\right) - 3.99 \left(\frac{L_{Down}}{D}\right) - 2.71 \left(\frac{S}{D}\right)^2 + .81 \left(\frac{L_{Down}}{D}\right)^2 - .41 \left(\frac{S}{D}\right) \left(\frac{L_{Down}}{D}\right) \quad (9.b)$$

$$Y_3 = 17.10 + .14 \left(\frac{L_{up}}{D}\right) - 4.80 \left(\frac{L_{Down}}{D}\right) - 0.41 \left(\frac{L_{up}}{D}\right)^2 + .81 \left(\frac{L_{Down}}{D}\right)^2 + .15 \left(\frac{L_{up}}{D}\right) \left(\frac{L_{Down}}{D}\right) \quad (9.c)$$

$$Y_4 = 5.04 + 10.70 \left(\frac{S}{D}\right) - 13.72 \left(\frac{D_e}{D}\right) - 2.71 \left(\frac{S}{D}\right)^2 + 13.68 \left(\frac{D_e}{D}\right)^2 - 1.52 \left(\frac{S}{D}\right) \left(\frac{D_e}{D}\right) \quad (9.d)$$

$$Y_5 = 0.939 - 0.082 Y_1 - 0.090 Y_2 + 0.0037 Y_1^2 + 0.0040 Y_2^2 + 0.0908 Y_1 \cdot Y_2 \quad (9.e)$$

$$Y_6 = 0.934 - 0.0847 Y_3 - 0.0876 Y_4 + 0.0038 Y_3^2 + 0.0039 Y_4^2 + 0.0908 Y_3 \cdot Y_4 \quad (9.f)$$

$$\frac{\Delta P}{\frac{1}{2} \rho V^2} = 0.0308 + 0.520 Y_5 + 0.473 Y_6 + 0.682 Y_5^2 + 0.685 Y_6^2 - 1.368 Y_5 \cdot Y_6 \quad (9.g)$$

Similarly, the corresponding polynomial representation of the model for the collection efficiency is in the following form:

$$Y'_1 = 103.6 - 197.9 \left(\frac{D_e}{D}\right) - 2.67 \left(\frac{L_{up}}{D}\right) + 211.3 \left(\frac{D_e}{D}\right)^2 + 0.04 \left(\frac{L_{up}}{D}\right)^2 + 1.18 \left(\frac{D_e}{D}\right) \left(\frac{L_{up}}{D}\right) \quad (10.a)$$

$$Y'_2 = 51.7 + 21.5 \left(\frac{S}{D}\right) + 5.72 \left(\frac{L_{Down}}{D}\right) - 2.92 \left(\frac{S}{D}\right)^2 - 3.92 \left(\frac{L_{Down}}{D}\right)^2 - 1.83 \left(\frac{S}{D}\right) \left(\frac{L_{Down}}{D}\right) \quad (10.b)$$

$$Y'_3 = 79.54 - 2.91 \left(\frac{L_{up}}{D}\right) + 2.68 \left(\frac{L_{Down}}{D}\right) + .045 \left(\frac{L_{up}}{D}\right)^2 - 3.92 \left(\frac{L_{Down}}{D}\right)^2 + 3.6 \left(\frac{L_{up}}{D}\right) \left(\frac{L_{Down}}{D}\right) \quad (10.c)$$

$$Y'_4 = 77.85 + 20.29 \left(\frac{S}{D}\right) - 188.0 \left(\frac{D_e}{D}\right) - 2.92 \left(\frac{S}{D}\right)^2 + 211.3 \left(\frac{D_e}{D}\right)^2 - 5.961 \left(\frac{S}{D}\right) \left(\frac{D_e}{D}\right) \quad (10.d)$$

$$Y'_5 = 3.8978 - 0.1041 Y'_1 - 0.0123 Y'_2 + 0.00071 Y_1'^2 + 9.521e - 5 Y_2'^2 + 0.01512 Y_1' \cdot Y_2' \quad (10.e)$$

$$Y'_6 = 7.1521 - 0.00712 Y'_3 - 0.20612 Y'_4 + 5.51e - 5 Y_3'^2 + 0.0015 Y_4'^2 + 0.015 Y_3' \cdot Y_4' \quad (10.f)$$

$$\eta = 0.17911 + 1.37011 Y'_5 - 0.3763 Y'_6 + 0.1042 Y_5'^2 + 0.11401 Y_6'^2 - 0.219 Y_5' \cdot Y_6' \quad (10.g)$$

The appropriate behavior of such GMDH type neural network model for the pressure drop is also depicted in Figure 8 for the training and testing data. Such behavior has also been shown for the training and testing data of efficiency in Figure 9. It is evident that the evolved GMDH type neural network in terms of simple polynomial equations successfully model and predict the outputs of the testing data that have not been used during the training process. To determine the accuracy of GMDH modeling, we also use a criterion, namely, Root Mean Square Error (RMSE) which demonstrates the difference between CFD data and GMDH predicted data and can be calculated as follows:

$$RMSE = \left(\frac{\sum |f_{CFD} - f_{GMDH}|^2}{N} \right)^{\frac{1}{2}} \quad (11)$$

where N is the pattern number and f is Δp or η . The comparison of RMSE for the training and testing data of the objective functions are shown in Table 5. As seen, the GMDH-type neural network predicts the objective functions with the acceptable deviation from CFD data. It should be noted that these polynomials are valid just for the design variables in the range of the present case study (Table 3). The models obtained in this section can now be utilized in the Pareto of the multi-objective optimization algorithm of the cyclone separators considering both the pressure drop and efficiency as the conflicting objectives. Such study may unveil some interesting and important optimal design principles that would not have been obtained without the use of a multi-objective optimization approach.

4. THE PARTICLE SWARM OPTIMIZATION HYBRIDIZED WITH MULTIPLE Crossover AND MUTATION OPERATOR

To overcome complexity and dimensionality of real-world problems, it is needed to improve the efficiency and accuracy of PSO. Therefore, to improve the performance of PSO in this paper, it is combined with the multiple crossover and mutation operator to update the particles' position. In this method, the multiple crossovers are developed to modify the converging process; and also the mutation operator is used to leap from any possible local optima. In the following, the concepts of the PSO, multiple crossover and mutation operator are introduced and in the next section, the hybrid of these operators is described.

4. 1. The Concept of Particle Swarm Optimization
Kennedy et al. [15] originally proposed the PSO algorithm for optimization. PSO is a population-based search algorithm based on the simulation of the social behavior of birds within a flock. Although originally adopted for balancing weights in neural networks [31],

PSO soon became a very popular global optimizer, mainly in problems in which the decision variables are real numbers [32-33].

TABLE 5. The comparison of RMSE for objective functions.

Objective Function	Train	Test
Δp	0.08132	0.0731
η	1.03701	1.0011

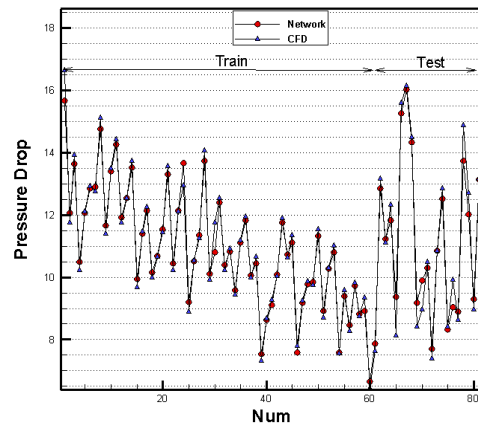


Figure 8. The behavior of GMDH type neural network model for the pressure drop of the training and testing data.

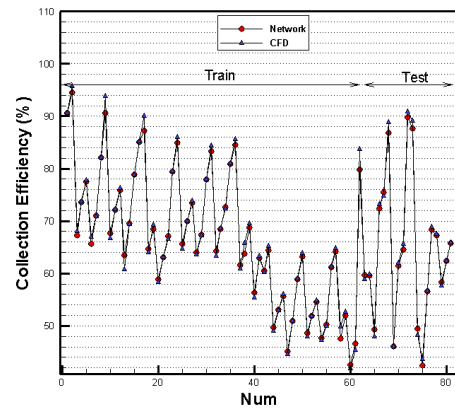


Figure 9. The behavior of GMDH type neural network model for the efficiency of the training and testing data.

In PSO, particles are “flown” through the hyper-dimensional search space. Changes to the position of the particles within the search space are based on the social-psychological tendency of the individuals to emulate the success of other individuals. The position of each particle is changed according to its own experience and that of its neighbors. Let $\vec{x}_i(t)$ denote the position of particle p_i , at time step t . The position of p_i is then

changed by adding a velocity $\vec{v}_i(t)$ to the current position, i.e.:

$$\vec{x}_i(t+1) = \vec{x}_i(t) + \vec{v}_i(t+1) \tag{12}$$

The velocity vector reflects the socially exchanged information and, in general, is defined as the following formula:

$$\vec{v}_i(t+1) = W \vec{v}_i(t) + Cr (\vec{x}_{global\ best} - \vec{x}_i(t)) \tag{13}$$

where $r \in [0,1]$ is a random value, C is the social learning factor and represents the attraction that a particle has toward the success of its neighbors, W is the inertia weight which is employed to control the impact of the previous history of velocities on the current velocity of a given particle. $\vec{x}_{global\ best}$ is the position of the best particle of the entire swarm [34].

4. 2. The Concept of the Multiple Crossovers and Mutation Operator

4. 2. 1. The Multiple Crossovers Unlike the traditional crossover using only two chromosomes, a crossover formula that contains three parent chromosomes is used in this study. We assume that chromosome $\vec{x}_i(t)$ is randomly selected from the population. Also, let $\rho \in [0, 1]$ be a random number. If $\rho < p_{Crossover}$, then the following multiple crossovers are performed to generate a new chromosome,

$$\vec{x}_i(t) = \vec{x}_i(t) + \sigma(2\vec{x}_i(t) - \vec{x}_{i-1}(t) - \vec{x}_{i-2}(t)) \tag{14}$$

where $\sigma \in [0,1]$ is a random value. If $\rho \geq p_{Crossover}$, the crossover operation is not performed.

4. 2. 2. The Mutation Operator The mutation operator provides a possible mutation on some chosen chromosomes $\vec{x}_i(t)$. Also, let $\vartheta \in [0,1]$ be a random number. If $\vartheta < p_{Mutation}$, then the following mutation operator is performed to generate a new chromosome,

$$\vec{x}_i(t) = \vec{x}_i(t) + \xi \times \kappa \tag{15}$$

where $\xi \in [0,1]$ is a random value and κ is a positive constant. If $\vartheta \geq p_{Mutation}$, no crossover operation is performed.

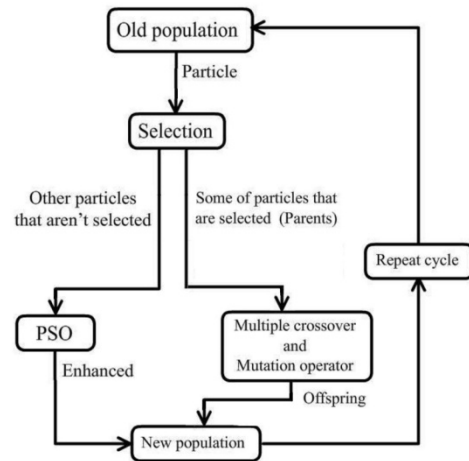


Figure 10. The flow chart of the hybrid of PSO, multiple crossovers and mutation operator.

4. 3. The Hybrid of PSO, Multiple Crossover and Mutation Operator

The flow chart of the hybrid of PSO, multiple crossover and mutation operator is shown in Figure 10. In the start of each iteration, two random numbers between zero and one are considered (ρ and ϑ) for each particle. If $\rho < p_{Crossover}$ or $\vartheta < p_{Mutation}$, then the multiple crossovers or the mutation operator will be performed respectively. However, if $\rho \geq p_{Crossover}$ and $\vartheta \geq p_{Mutation}$, this particle will be enhanced by PSO.

4. 4. The Hybrid of PSO and Multiple Crossovers and Mutation Operator for Multi-Objective Problems

Optimization problems that have more than one objective function are common in every field or area of knowledge. In such problems, the objectives conflicting with each other are optimized normally, which means that there is no single solution for these problems. Instead, we aim to find proper "trade-off" solutions that represent the best possible compromises among the objectives. PSO is a heuristic search technique [17] that simulates the movements of a flock of birds which aim to find food. The relative simplicity of PSO and the fact that it is a population-based technique have made it a natural candidate extended for multi-objective optimization. Moore and Chapman proposed the first extension of the PSO strategy for solving multi-objective problems in an unpublished manuscript in 1999 [35]. After this early attempt, a great interest in extending PSO has been aroused among researchers, but interestingly, the next proposal was not published until 2002. Nevertheless, there are currently different proposals of multi-objective PSOs reported in

the specialized literature. The problems are of the following type :

$$\text{Minimize } \vec{f}(\vec{x}) := [f_1(\vec{x}), f_2(\vec{x}), \dots, f_k(\vec{x})] \tag{16}$$

Subject to:

$$g_i(\vec{x}) \leq 0 \quad i=1,2,\dots,m \tag{17}$$

$$h_i(\vec{x}) = 0 \quad i=1,2,\dots,p \tag{18}$$

where $\vec{x} = [x_1, x_2, \dots, x_n]^T$ is the vector of decision variables, $f_i: R^n \rightarrow R, i=1, \dots, k$ are the objective functions and $g_i, h_j: R^n \rightarrow R, i=1, \dots, m, j=1, \dots, p$ the constraint functions of the problem. To describe the concept of optimality, we will introduce next a few definitions, as follows:

- **Dominance:** Given two vectors $\vec{x}, \vec{y} \in R^k$ we say that $\vec{x} \leq \vec{y}$ if $\vec{x}_i \leq \vec{y}_i$ for $i=1, \dots, n$ and that \vec{x} dominates \vec{y} (denoted by $\vec{x} \prec \vec{y}$) if $\vec{x} \leq \vec{y}$ and $\vec{x} \neq \vec{y}$.
- **Non-Dominance:** We say that a vector of decision variables $\vec{x} \in \chi \subset R^n$ is non-dominated with respect to χ , if there does not exist another $\vec{x}' \in \chi$ such that $\vec{f}(\vec{x}') \prec \vec{f}(\vec{x})$.
- **Pareto-optimal:** We say that a vector of decision variables $\vec{x}^* \in F \subset R^n$ (F is the feasible region) is Pareto-optimal if it is non-dominated with respect to F .
- **Pareto Optimal Set:** The Pareto-optimal Set p^* is defined by: $p^* = \{\vec{x} \in F \mid \vec{x} \text{ is pareto-optimal}\}$.
- **Pareto Front:** The Pareto Front pF^* is defined by: $pF^* = \{\vec{f}(\vec{x}) \in R^k \mid \vec{x} \in p^*\}$.

Thus, the Pareto optimal set of the set F of all the decision variable vectors are determined in such a way that satisfies Equations (16) and (17). However, note that all the Pareto optimal set is not normally desirable or achievable in practice (e.g., it may not be desirable to have different solutions that map to the same values in the objective function space). In order to apply the PSO strategy for solving multi-objective optimization problems, the original scheme obviously has to be modified. The solution set of a problem with multiple objectives does not consist of a single solution (in the global optimization). Instead, in multi-objective optimization, we aim to find a set of different solutions (the so-called Pareto optimal set). When solving single-

objective optimization problems, $\vec{x}_{global \ best}$ is used as a leader to update particles' position. However, in the case of multi-objective optimization problems, each particle might have a set of different leaders from which just one can be selected in order to update its position. Such a set of leaders is usually stored in a different place from the swarm, that we will call "external archive": This is a repository in which the non-dominated solutions found so far are stored. However, if all non-dominated solutions are retained in the archive, then the size of the archive increases very quickly. This is an important issue because the archive has to be updated at each generation. Thus, this update may become very expensive, computationally, if the size of the archive grows too much. Therefore, the archive tends to be bounded, which makes necessary the use of an additional criterion to decide which non-dominated solutions to retain.

In this paper, it is an adopted ϵ -elimination technique to prune the archive. In this approach, the entire particles in the archive have a neighborhood radius that is equal to ϵ and if a particle has a distance fewer than ϵ to another, the particle will be eliminated in the objective function space. Here, the following equation is used to determine ϵ :

$$\epsilon = \frac{t}{\sigma \times \text{maximum generation}} \tag{19}$$

where t is the time step and σ is a positive constant. The contents of the external archive are also reported as the final output of the algorithm. In this paper, we describe a leader selection technique that is based on the density measures. For this propose, a neighborhood radius for each particle in archive is defined. Then, the number of these particles' neighborhoods is calculated in the objective function space. The particle that has fewer number of neighborhood is preferred as leader.

5. MULTI-OBJECTIVE OPTIMIZATION OF CYCLONE SEPARATORS USING THE HYBRID OF PSO, MULTIPLE CROSSOVERS AND MUTATION OPERATOR

In order to investigate the optimal performance of the cyclone separators in different geometrical parameters, the polynomial neural network models obtained in Section 3 are now deployed in a multi-objective optimization procedure. In the MO hybrid algorithm, the inertia weight W is nonlinearly decreased over time by the following equation:

$$W = W_1 - (W_1 - W_2) \times \left(\frac{t}{\text{maximum generation}}\right)^{0.5} \tag{20}$$

and C is nonlinearly increased over time as follows:

$$C = C_i - (C_i - C_f) \times \left(\frac{t}{\text{maximum generation}} \right)^2 \quad (21)$$

where $W_1 = 0.75, W_2 = 0.25, C_i = 0,$ and $C_f = 2.5$. The related variables used in the multiple crossovers and mutation operator are: $p_{\text{Crossover}} = 0.7, p_{\text{Mutation}} = 0.2,$ and $\kappa = 0.05$. Furthermore, the term $\vec{v}_i(t)$ is limited to the range $[-1,+1]$ and if the velocity violates this range, a random number from $[0,1]$ is multiplied by it. Based on the observation of the movement of the Pareto front, the population size is set to 100 and the maximum iteration is also set to 100. The two conflicting objectives in this study are Δp and η which have to be simultaneously optimized with respect to the design variables $(S/D), (D_c/D), (L_{up}/D)$ and (L_{Down}/D) . The multi-objective optimization problem can be formulated in the following form:

$$\left\{ \begin{array}{l} \text{Maximize the Collection Efficiency } (\eta) = f_1 \left(\frac{S}{D}, \frac{D_c}{D}, \frac{L_{up}}{D}, \frac{L_{Down}}{D} \right) \\ \text{Minimize the Pressure Drop } (\Delta p) = f_2 \left(\frac{S}{D}, \frac{D_c}{D}, \frac{L_{up}}{D}, \frac{L_{Down}}{D} \right) \\ \text{Subject to } 0.9 \leq x_1 = \frac{S}{D} \leq 1.725 \\ 0.125 \leq x_2 = \frac{D_c}{D} \leq 0.6 \\ 0.875 \leq x_3 = \frac{L_{up}}{D} \leq 2.775 \\ 0.875 \leq x_4 = \frac{L_{Down}}{D} \leq 2.775 \end{array} \right. \quad (22)$$

The variable in Equation (22) is the maximum or minimum value having a standard cyclone. Figure 11 depicts the obtained non-dominated optimum design points as a Pareto front of those two objective functions. There are five optimum design points, namely, A, B, C, D and E whose corresponding design variables and objective functions are shown in Table 6. These points clearly demonstrate tradeoffs in objective functions, pressure drop and collection efficiency, from which an appropriate design can be compromisingly chosen. It is clear from Figure 11 that all the optimum design points in the Pareto front are non-dominated and could be chosen by a designer as an optimum cyclone separator. Evidently, choosing a better value for any objective function in the Pareto front would cause a worse value for another objective. The corresponding decision variables of the Pareto front shown in Figure 11 are the best possible design points so that if any other set of decision variables is chosen, the corresponding values of the pair of objectives will locate a point inferior to this Pareto front. In fact, such inferior area in the space of the two objectives is bottom/right side of Figure 11. In Figure 11, the design points A and E stand for the

best pressure drop and the best collection efficiency, respectively. Moreover, the other optimum design points, B and D can be simply recognized from Figure 11. The design point, B exhibits important optimal design concepts. In fact, optimum design point B obtained in this paper exhibits an increase in the pressure drop (about 6.1%) in comparison with that of point A, while its efficiency improves about 20.3 % in comparison with that of A. Similarly, optimum design point D exhibits a decrease in efficiency (about 14.5%) in comparison with that of point E, while its pressure drop improves about 38 % in comparison with that of E. Table 6 shows the maximum and minimum collection efficiency obtained from the minimum and maximum of $(D_c/D), (L_{up}/D),$ and (L_{Down}/D) . These results are compatible with those of Zhu et al. [4] and Lim et al. [36]. It means that a decrease in $D_c/D, L_{up}/D,$ and L_{Down}/D leads to an increase in the collection efficiency and pressure drop. It is now desired to find a trade-off optimum design point compromising both objective functions. This can be achieved by the method employed in this paper, namely, the mapping method (normalization method).

TABLE 6. The values of objective functions and their associated design variables of the optimum points.

Point	S/D	D _c /D	L _{up} /D	L _{Down} /D	Δp / .5ρ v ²	η (%)
A	0.900	0.500	2.775	2.775	6.475	45.549
B	0.900	0.600	2.775	2.011	7.076	56.095
C	1.170	0.125	2.775	1.297	9.831	79.990
D	1.725	0.125	2.775	0.905	12.516	89.374
E	1.725	0.125	0.900	0.875	16.277	97.138

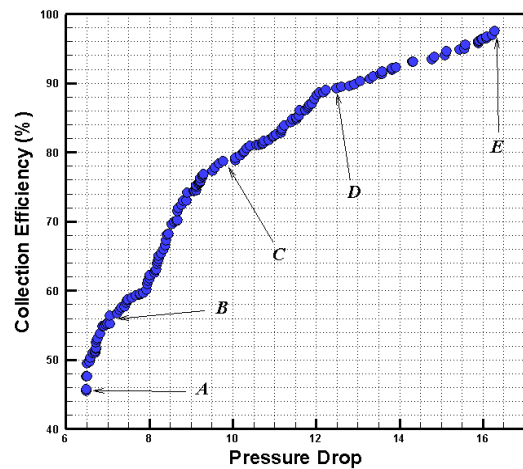


Figure 11. The obtained non-dominated optimum design points as a Pareto front of those two objective functions based on proposed hybrid algorithm.

In this method, the values of objective functions of all non-dominated points are mapped into interval 0 and 1. Using the sum of these values for each non-dominated point, the trade-off point simply is one having the minimum sum of those values. Consequently, optimum design point *C* is the trade-off point obtained from the mapping method.

The Pareto front obtained from the proposed method (Figure 11) has been superimposed with the Pareto front of multi-objective genetic algorithm, NSGA II [37], and the corresponding CFD simulation results in Figure 12. It can be clearly seen from this figure that the proposed Pareto front lies on the best possible combination of the objective values of CFD data and achieves better objective functions than NSGA II for the present case study (cyclone separators), which demonstrate the effectiveness of this investigation in obtaining the optimal Pareto front.

In a post numerical study, the design points of the obtained Pareto front have been re-evaluated by CFD. It should be noted that the optimum design points of the MOPSO method are not included in the training and testing sets using GMDH-type neural network which makes such re-evaluation sensible. The results of such CFD analysis re-evaluations have been compared with those of numerical results using GMDH polynomials in Table 7. As seen, the optimum GMDH data agree well with the CFD results. Shi et al. [38] found that for the optimization problems with a large number of parameters and objective functions, a limited number of CFD evaluations are not sufficient. However, such a good agreement between network and CFD re-evaluation data in this paper is due to the large number of CFD simulations.

In fact, we have studied a problem with two objective functions and four design variables with 81 different designs which are sufficient to cover the domain of different designs.

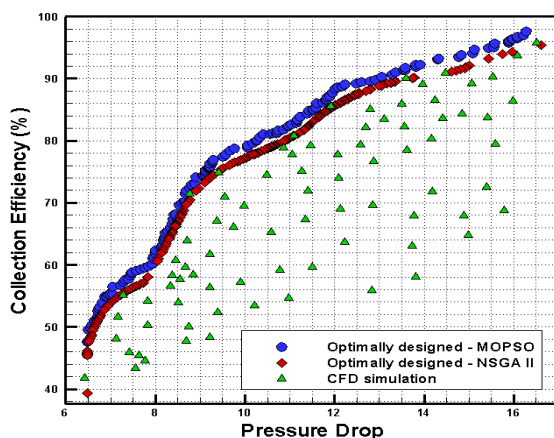


Figure 12. The comparison among the Pareto front obtained from the proposed method, NSGA II, and the corresponding CFD simulation results.

TABLE 7. Re-evaluation of the obtained optimal Pareto front using CFD.

Points	$\Delta p / .5\rho v^2$			η (%)		
	GMDH	CFD	Error (%)	GMDH	CFD	Error (%)
A	6.475	6.201	-4.41	45.549	43.234	-5.35
B	7.076	6.821	-3.73	56.095	53.919	-3.89
C	9.831	10.042	2.10	79.990	82.030	2.56
D	12.516	12.933	3.22	89.374	92.851	3.77
E	16.277	16.090	-1.16	97.138	98.336	1.35

6. CONCLUSION

Two different polynomial relations for the collection efficiency and pressure drop have been found by evolved GS-GMDH type neural networks using some experimentally validated CFD simulations for input-output data of the cyclone separators. The derived polynomial models have been used in the MOPSO optimization process; therefore, some interesting informative optimum design aspects have been revealed for the cyclones. The Pareto front of the hybrid of MOPSO and NSGA II methods have been compared. It was illustrated that MOPSO Pareto front lies on the best possible combination of the objective values of CFD data and achieves better objective functions than NSGA II for the present case study.

7. REFERENCES

1. Stairmand, C. J., "The design and performance of cyclone separators", *Transactions of Institute of Chemical Engineers*, Vol. 29, No., (1951), 356-383.
2. Dirgo, J. and Leith, D., "Performance of theoretically optimised cyclones", *Filtration & Separation*, Vol. 22, No. 2, (1985), 119-125.
3. Cheremisinoff, P. N., "Air pollution control and design for industry", CRC Press, (1993).
4. Zhu, Y. and Lee, K., "Experimental study on small cyclones operating at high flowrates", *Journal of Aerosol Science*, Vol. 30, No. 10, (1999), 1303-1315.
5. Ravi, G., Gupta, S. K. and Ray, M., "Multiobjective optimization of cyclone separators using genetic algorithm", *Industrial & Engineering Chemistry Research*, Vol. 39, No. 11, (2000), 4272-4286.
6. Xiang, R., Park, S. and Lee, K., "Effects of cone dimension on cyclone performance", *Journal of Aerosol Science*, Vol. 32, No. 4, (2001), 549-561.
7. Shalaby, H., Wozniak, K. and Wozniak, G., "Numerical calculation of particle-laden cyclone separator flow using les", *Engineering Applications of Computational Fluid Mechanics*, Vol. 2, No. 4, (2008), 382-392.
8. Safikhani, H., Shams, M. and Dashti, S., "Numerical simulation of square cyclones in small sizes", *Advanced Powder Technology*, Vol. 22, No. 3, (2011), 359-365.

9. Safikhani, H., Hajiloo, A. and Ranjbar, M., "Modeling and multi-objective optimization of cyclone separators using cfd and genetic algorithms", *Computers & Chemical Engineering*, Vol. 35, No. 6, (2011), 1064-1071.
10. Åström, K. and Eykhoff, P., "System identification—a survey", *Automatica*, Vol. 7, No. 2, (1971), 123-162.
11. Sanchez, E., Shibata, T. and Zadeh, L. A., "Genetic algorithms and fuzzy logic systems: Soft computing perspectives", *World Scientific*, Vol. 7, (1997).
12. Kristinsson, K. and Dumont, G. A., "System identification and control using genetic algorithms", *Systems, Man and Cybernetics, IEEE Transactions on*, Vol. 22, No. 5, (1992), 1033-1046.
13. Ivakhnenko, A., "Polynomial theory of complex systems", *Systems, Man and Cybernetics, IEEE Transactions on*, Vol., No. 4, (1971), 364-378.
14. Farlow, S. J., "Self-organizing methods in modeling: Gmdh type algorithms", CrC Press, Vol. 54, (1984).
15. Kennedy, J., "Particle swarm optimization, in Encyclopedia of machine learning", , Springer, (2010), 760-766.
16. Angelina, P. J., "Using selection to improve particle swarm optimization", in Evolutionary Computation Proceedings, 1998. IEEE World Congress on Computational Intelligence., The 1998 IEEE International Conference on, IEEE. (1998), 84-89.
17. Eberhart, R. C. and Shi, Y., "Comparison between genetic algorithms and particle swarm optimization", in Evolutionary Programming VII, Springer. (1998), 611-616.
18. Yoshida, H., Kawata, K., Fukuyama, Y., Takayama, S. and Nakanishi, Y., "A particle swarm optimization for reactive power and voltage control considering voltage security assessment", *Power Systems, IEEE Transactions on*, Vol. 15, No. 4, (2000), 1232-1239.
19. Rahimi-Vahed, A., Mirghorbani, S. and Rabbani, M., "A hybrid multi-objective particle swarm algorithm for a mixed-model assembly line sequencing problem", *Engineering Optimization*, Vol. 39, No. 8, (2007), 877-898.
20. Janga Reddy, M. and Nagesh Kumar, D., "An efficient multi-objective optimization algorithm based on swarm intelligence for engineering design", *Engineering Optimization*, Vol. 39, No. 1, (2007), 49-68.
21. Annamdas, K. K. and Rao, S. S., "Multi-objective optimization of engineering systems using game theory and particle swarm optimization", *Engineering Optimization*, Vol. 41, No. 8, (2009), 737-752.
22. Safikhani, H., Akhavan-Behabadi, M., Shams, M. and Rahimyan, M., "Numerical simulation of flow field in three types of standard cyclone separators", *Advanced Powder Technology*, Vol. 21, No. 4, (2010), 435-442.
23. Raoufi, A., Shams, M. and Kanani, H., "Cfd analysis of flow field in square cyclones", *Powder Technology*, Vol. 191, No. 3, (2009), 349-357.
24. Cooper, C. D. and Alley, F. C., "Air pollution control: A design approach", Waveland Press Long Grove, Ill, Vol. 2, (2002).
25. Casal, J. and Martinez-Benet, J. M., "Better way to calculate cyclone pressure drop", *Chemical Engineering*, Vol. 90, No. 2, (1983), 99-100.
26. Coker, A., "Understand cyclone design", *Chemical Engineering Progress;(United States)*, Vol. 89, No. 12, (1993).
27. Wang, L., "Theoretical study of cyclone design", Texas A&M University, (2004).
28. König, C., "Untersuchungen zum abscheideverhalten von geometrisch ähnlichen zyklonen", (1990).
29. Fraser, S., Abdel-Razek, A. and Abdullah, M., "Computational and experimental investigations in a cyclone dust separator", *Proceedings of the Institution of Mechanical Engineers, Part E: Journal of Process Mechanical Engineering*, Vol. 211, No. 4, (1997), 247-257.
30. Jamali, A., Nariman-Zadeh, N., Darvizeh, A., Masoumi, A. and Hamrang, S., "Multi-objective evolutionary optimization of polynomial neural networks for modelling and prediction of explosive cutting process", *Engineering Applications of Artificial Intelligence*, Vol. 22, No. 4, (2009), 676-687.
31. Eberhart, R., Simpson, P. and Dobbins, R., "Computational intelligence pc tools", Academic Press Professional, Inc., (1996).
32. Engelbrecht, A. P., "Computational intelligence: An introduction", Wiley. com, (2007).
33. Engelbrecht, A. P., "Fundamentals of computational swarm intelligence", Wiley Chichester, Vol. 1, (2005).
34. Chau, K., "Application of a pso-based neural network in analysis of outcomes of construction claims", *Automation in Construction*, Vol. 16, No. 5, (2007), 642-646.
35. Moore, J. and Chapman, R., "Application of particle swarm to multiobjective optimization", *Department of Computer Science and Software Engineering, Auburn University*, (1999).
36. Lim, K., Kim, H. and Lee, K., "Characteristics of the collection efficiency for a cyclone with different vortex finder shapes", *Journal of Aerosol Science*, Vol. 35, No. 6, (2004), 743-754.
37. Deb, K., Pratap, A., Agarwal, S. and Meyarivan, T., "A fast and elitist multiobjective genetic algorithm: Nsga-ii", *Evolutionary Computation, IEEE Transactions on*, Vol. 6, No. 2, (2002), 182-197.
38. Shi, Y. and Reitz, R. D., "Assessment of multiobjective genetic algorithms with different niching strategies and regression methods for engine optimization and design", *Journal of Engineering for Gas Turbines and Power*, Vol. 132, No. 5, (2010).

Modeling and Hybrid Pareto Optimization of Cyclone Separators Using Group Method of Data Handling (GMDH) and Particle Swarm Optimization (PSO)

M. J. Mahmoodabadi^a, M. Taherkhorsandi^b, H. Safikhani^c

^a Department of Mechanical Engineering, Sirjan University of Technology, Sirjan, Iran

^b Young Researchers Club, Rasht branch, Islamic Azad University, Rasht, Iran

^c Department of Mechanical Engineering, Amirkabir University of Technology, Tehran, Iran

PAPER INFO

چکیده

Paper history:

Received 05 January 2012

Accepted in revised form 30 August 2012

Keywords:

Two-phase Flow

Gas-solid

Particle Swarm Optimization

Multi-objective Optimization

GMDH

در این تحقیق، یک الگوریتم بهینه سازی چند هدفی سه مرحله‌ای برای جداکننده‌های سیکلونی و به منظور رسیدن به هدف‌های طراحی در نظر گرفته شده است. ابتدا افت فشار Δp و بازده مجموع η در یک مجموعه‌ی جداکننده‌ی سیکلونی به صورت عددی محاسبه می‌شود. سپس، دو مدل متا بر اساس شبه‌عصبی نوع GMDH برای مدل سازی Δp و η به عنوان توابع مورد نیاز و با توجه به ویژگی‌های هندسی در نظر گرفته شده است. از یک الگوریتم چند هدفی بر پایه‌ی بهینه سازی تجمعی ذره، ادغام چندگانه و عملگر جهش برای بهینه سازی پارتویی سیکلون‌ها و با توجه به دو تابع هدف متضاد استفاده شده است. با مقایسه نتایج بهینه‌سازی چندهدفه پارتویی دو مدل متا به دست آمده از MOPSO و الگوریتم ژنتیک چند هدفه NSGA II، روابط مهمی برای طراحی بهینه در عملکرد جداکننده‌های سیکلونی به دست آمده است.

doi: 10.5829/idosi.ije.2013.26.09c.15

